

Design of a Rotating Facility for Extracorporeal Treatment of an Explanted Liver with Disseminated Metastases by Boron Neutron Capture Therapy with an Epithermal Neutron Beam

V. A. Nievaart,^{a,b,1} R. L. Moss,^b J. L. Kloosterman,^a T. H. J. J. van der Hagen^{a,c} H. van Dam^a A. Wittig,^d M. Malago^e and W. Sauerwein^d

^a Department of Applied Sciences, Delft University of Technology, 2628CJ Delft, The Netherlands; ^b Joint Research Centre of the European Commission, 1755ZG Petten, The Netherlands; ^c Reactor Institute Delft, Delft University of Technology, 2629JB Delft, The Netherlands; ^d Clinic and Polyclinic for Radiotherapy, Essen University Hospital, 45122 Essen, Germany; and ^e Department of General and Transplantation Surgery, Essen University Hospital, 45122 Essen, Germany

Nievaart, V. A., Moss, R. L., Kloosterman, J. L., van der Hagen, T. H. J. J., van Dam, H., Wittig, A., Malago, M. and Sauerwein, W. Design of a Rotating Facility for Extracorporeal Treatment of an Explanted Liver with Disseminated Metastases by Boron Neutron Capture Therapy with an Epithermal Neutron Beam. *Radiat. Res.* 166, 81–88 (2006).

In 2001, at the TRIGA reactor of the University of Pavia (Italy), a patient suffering from diffuse liver metastases from an adenocarcinoma of the sigmoid was successfully treated by boron neutron capture therapy (BNCT). The procedure involved boron infusion prior to hepatectomy, irradiation of the explanted liver at the thermal column of the reactor, and subsequent reimplantation. A complete response was observed. This encouraging outcome stimulated the Essen/Petten BNCT group to investigate whether such an extracorporeal irradiation could be performed at the BNCT irradiation facility at the HFR Petten (The Netherlands), which has very different irradiation characteristics than the Pavia facility. A computational study has been carried out. A rotating PMMA container with a liver, surrounded by PMMA and graphite, is simulated using the Monte Carlo code MCNP. Due to the rotation and neutron moderation of the PMMA container, the initial epithermal neutron beam provides a nearly homogeneous thermal neutron field in the liver. The main conditions for treatment as reported from the Pavia experiment, i.e. a thermal neutron fluence of $4 \times 10^{12} \pm 20\% \text{ cm}^{-2}$, can be closely met at the HFR in an acceptable time, which, depending on the defined conditions, is between 140 and 180 min.

© 2006 by Radiation Research Society

INTRODUCTION

The liver is the first major organ reached by the blood draining the gastrointestinal tract. Consequently, it is a common site of hematogenous metastasis from gastrointes-

tinal malignancies. Colorectal cancer is the second leading cause of cancer-related death in developed countries. In the U.S. alone, 146,000 new cases occur annually (1), of which 50% develop liver metastases, and in a third of these, the liver will be the only site of metastases (2). Untreated hepatic colorectal metastasis has a poor prognosis, with a median survival of 6–12 months (3). In selected cases, surgery offers an effective therapeutic option leading to an improved median survival of 40 months or more and a 20% 10-year survival (3). However, in cases of multiple tumor lesions restricted to the liver that cannot be removed by partial hepatectomy, chemotherapy is the only treatment that can be offered. Even though the newest chemotherapeutic drugs have a response rate of around 40%, the overall survival benefit has been shown to be marginal. Thus attention has turned to loco-regional techniques that together with improved surgical procedures may be potentially curative. One such option could be the extracorporeal treatment of the liver by boron neutron capture therapy (BNCT).

The investigation presented here is motivated by a successful extracorporeal treatment using BNCT on one patient in Pavia (Italy) (4, 5). The 48-year-old patient developed synchronous diffuse liver metastases from an adenocarcinoma of the sigmoid colon; these liver metastases progressed after conventional chemotherapy. After intensive preclinical experiments (6, 7), the patient received 750 ml of a 0.14 M boronophenylalanine (BPA)-fructose solution (300 mg BPA per kg body weight) through the colic vein over a period of 2 h. After the infusion, tissue and tumor samples were taken to measure the boron-10 concentration just prior to hepatectomy. The explanted liver was cooled to 4°C and transported to the TRIGA reactor of the University of Pavia where it was irradiated at the thermal column for 11 min, producing a neutron fluence of $4 \times 10^{12} \pm 20\% \text{ cm}^{-2}$ (4).² After BNCT, the liver was transported back to the operating theater and reimplanted. A complete

¹ Address for correspondence: Joint Research Centre of the European Commission, P.O. Box 2, 1755ZG Petten, The Netherlands; e-mail: victor.nievaart@jrc.nl.

² Private communications with A. Zonta, T. Pinelli and S. Altieri.

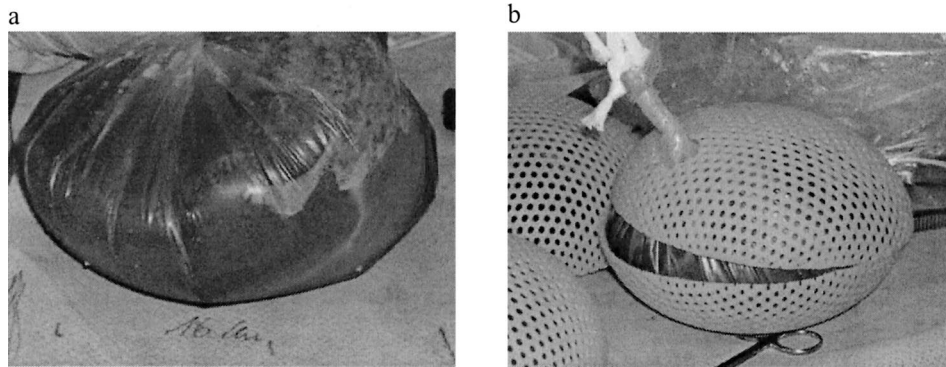


FIG. 1. Panel a: In a plastic bag, a liver takes the form of a spheroid. Panel b: Insertion of a discarded human liver into a custom-manufactured spheroid-shaped mold.

tumor response was observed. After an observation period of 12 months, a CT scan of the liver showed a normal liver without any residual lesions in the former tumor areas. After 20 months, a tumor recurrence was observed in the form of a nodule outside the liver but in the area of the former liver surgery. It was interpreted as iatrogenic due to the sampling of tumor tissue prior to the liver explantation and was surgically removed. An adjuvant chemotherapy was administered after this intervention. At 33 months after BNCT, an intrahepatic tumor was detected shortly followed by intraperitoneal spreading. The patient died in August 2005, 44 months after BNCT. A second patient suffering from diffuse liver metastases of a colorectal cancer was treated following the same procedure. He died 6 weeks after the auto-transplantation due to cardiac problems that were interpreted as complications from prior chemotherapy. The post mortem evaluation did not demonstrate any viable tumor in the liver (communication from A. Zonta).³

These observations stimulated not only the work presented here but also similar studies in Finland (8), Japan (9) and the U.S. (10).

BNCT uses the reaction that occurs between the boron-10 nucleus and thermal neutrons. In this reaction, the thermal neutron is captured by the nucleus, and the resulting boron-11 nucleus decays with the emission of high-LET and high-RBE α and ${}^7\text{Li}$ particles. The ranges of these particles are only 9 and 5 μm , respectively; thus, if either particle traverses the cell nucleus, it will lead to clonogenic death. With targeted delivery of ${}^{10}\text{B}$ to tumor cells, a selective destruction of these cells can be obtained (11). This principle offers the possibility to treat multiple metastases in the liver much more efficiently than with existing conventional therapies. Moreover, BNCT has the potential to eliminate very small metastases or satellite nodules that are not clinically detectable and are often responsible for recurrent disease. A prerequisite, however, is the selective accumulation of ${}^{10}\text{B}$ inside the tumor cells. Such an uptake can be expected using the boron compound BPA, which is

actively transported by the L-amino acid transport system into cells (12) and which is already used in clinical trials (13–18). Another precondition is the delivery of a sufficient number of thermal neutrons to the tumor cells. This last aspect will be the focus of this paper. The proposed irradiations will take place at the BNCT facility (19) of the High Flux Reactor (HFR) in Petten (The Netherlands), using the available, well-collimated epithermal neutron beam. The aim of the study is therefore to demonstrate that a homogeneous thermal neutron flux distribution can be delivered to the liver using a directed epithermal neutron beam. The ability to generate a homogeneous thermal neutron flux will open up the possibility to treat liver cancers at other BNCT facilities.

MATERIALS AND METHODS

The Liver

The liver is the largest internal organ in the human body and can be characterized as a spongy, wedge-shaped organ. According to the literature (20), the average weight of a healthy male liver is around 1.5 kg and that of a healthy female liver is 1.3 kg. The maximum dimensions, when in the body, are up to 22.5 cm transversally, and vertically, near its lateral or right surface, up to 17.5 cm, the greatest anterior-posterior diameter is 12.5 cm. A liver with metastases may have a larger size and volume. However, the evolving calculations, which are reported later, suggest that a more homogeneous dose distribution would be possible with a spheroid-shaped volume. A liver can readily be molded into a spheroidal shape, as illustrated in Fig. 1a, when it is placed in a plastic bag, as is usually done for the transport of an explanted liver. Figure 1b may clarify this approach; a female liver of 1.3 kg fits perfectly into a spheroid-shaped mold with a volume of 1.6 liters.

The pictures were taken in the operating theatre of the Department of General and Transplantation Surgery at the University Hospital Essen (Germany) after de-identification and prior to the discarding of an explanted liver and are therefore, under German law, exempt from review for protection of the welfare of human subjects.

Medical Requirements

The University Hospital Essen is one of the main European centers for both diseased and living donor liver transplantation (21).⁴ It is collabo-

³ Europhysics Conference on New Trends in Nuclear Physics and Technologies. September 5–9, Pavia, Italy, 2005.

⁴ <http://www.dso.de/grafiken/g48.html>.

rating and participating in the preparation of extracorporeal BNCT at the HFR Petten, followed by auto-transplantation in Essen.

The time that the organ can be maintained outside the body and the time the anhepatic patient can be maintained are critical issues. In our initial evaluations, the time the liver is allowed to be outside the operating theatre will be defined as 6 h. Using routine means of transport for organs, the liver can be transported from the operating theatre in Essen to the irradiation room at the HFR within 1 h. The time remaining for the setup at the irradiation facility and irradiation procedure, no more than 4 h, seems to be acceptable. After explantation, during transport and irradiation, the liver must be maintained constantly at a controlled temperature of 4°C. The liver is a flexible organ; however, it should not suffer from pressure or other mechanical injury.

Radiation Components in BNCT

In BNCT, the absorbed dose in the irradiated volume results from several dose components, some transported in the tissue by the incident beam, others generated in the irradiated volume by nuclear reactions. The four dose components that must be evaluated are the boron dose (D_B), the thermal and fast-neutron doses (D_p and D_n), and the γ -ray dose (D_γ) (22). To handle these different dose components and to take into consideration the different biological effectiveness, the term total biologically weighted dose, D_w , has been proposed.⁵ Pinelli *et al.* estimated the limiting dose to the liver to be $D_w = 15$ Gy (23) when applying the weighting factors originating from *in vitro* and *in vivo* experiments on the central nervous system and skin (24–26). Apart from the fact that the weighting factors for an explanted liver irradiated in hypoxia at a temperature of 4°C are not known, this computational study nevertheless follows the proposal of Pinelli. This approach should be seen as an approximation. The limiting tolerable dose needs to be established through appropriate animal experiments.

It has to be stressed that only the boron dose component is “targeted” to the tumor. All other dose components are not tumor specific and produce an absorbed dose in the healthy parts of the liver; i.e., they determine the limiting dose that can be given to the organ.

Successful BNCT depends on two factors: the minimization of the non-specific dose components and the differential boron uptake in healthy liver tissue and metastases. The latter is important since the uptake and distribution will probably vary between livers and must be evaluated for each clinical case; this is currently being studied in an ongoing trial.⁶

Irradiation Goals and Limits in this Computational Study

The main goal of this study is to evaluate and compare the fluence in the Petten setup as that reported in Pavia. Nevertheless, the total weighted dose D_w will be compared to that reported in Pavia using the estimates described above. For the first patient, Pinelli *et al.* (4) report a D_w of 8.6 ± 0.5 Gy in the healthy liver with a ^{10}B concentration of 8 ppm and a D_w of 62 ± 2 Gy in the tumors with a ^{10}B concentration of 47 ppm. Since the metastases are spread throughout the liver, the thermal neutron flux distribution should be as homogeneous as possible.

Rotating Liver

When dealing with a thermal column, as in the Pavia setup, the optimum position for the liver is in its natural form when placed on a flat surface. A thermal column allows for the organ to be placed in effectively a “cloud” of thermal neutrons. The thermal neutron flux will be a maximum at the surface and will decay rather strongly into the liver. Around 3 cm from the surface, the thermal neutron flux will be only half the

⁵ IAEA, Current status of neutron capture therapy. IAEA-TECDOC-1223, Vienna, 2001.

⁶ EORTC protocol 11001 (April 29, 2003): ^{10}B -uptake in different tumours using the boron compounds BSH and BPA. Study coordinator: W. Sauerwein.

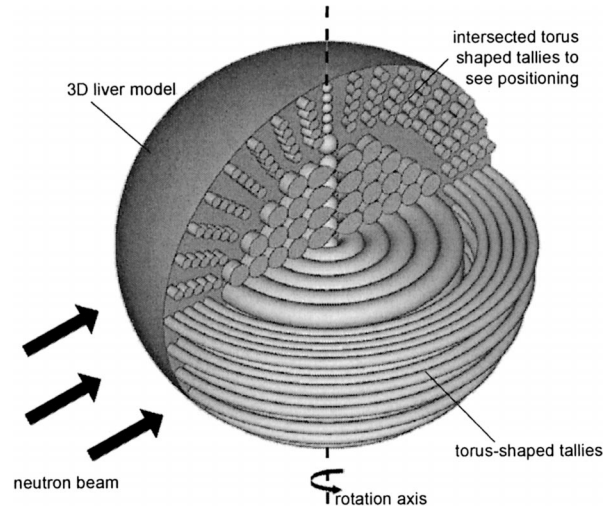


FIG. 2. Isometric view of the spheroidal liver model, which contains torus-shaped tallies to simulate rotation. With several tori, the flux in the whole liver can be determined.

maximum (surface) value. An initial design considered fitting the liver into an imaginary cylindrical container with a diameter of 25 cm and a height of 8 cm. In this way, the thermal neutrons, coming from both sides, will deliver a homogeneously distributed dose in the liver.

When dealing with an epithermal neutron beam, the setup must be completely re-evaluated. With respect to the Petten beam, the neutron energy spectrum consists mainly of epithermal neutrons with energies mainly between 1 eV and 10 keV, with two small peaks around 30 keV and 70 keV. The beam is “highly directed”, has a very small divergence (2°), and is circular due to beam collimators of diameters 8, 12 and 15 cm. The thermal neutron flux caused by moderation of the epithermal neutrons has a maximum at 3 cm from the surface and is half this maximum value at 0.5 cm and 6.5 cm. After some initial studies, including the cylindrical approach as mentioned above, it became apparent that the most effective part of the neutron fluence, i.e. between 0.5 cm and 6.5 cm, can be used if the liver is inserted into a spheroid-shaped container and then rotated around the polar axis. In this way, when the thermal maximum is moved slightly nearer to the surface by the scattering properties of the container material, the thermal fluence will be spread over the liver volume. At the center of the spheroid, the thermal fluence is at its lowest but, at the same time, is distributed over a smaller volume when rotating.

When using one of the currently available treatment planning programs designed for BNCT, such as BNCT_rtpc (27), SERA (28) or NCTPlan (29), it is not possible to simulate rotating bodies and to calculate the overall thermal neutron fluence distribution. It was therefore necessary to carry out the study using the Monte Carlo code MCNP (30). To calculate the neutron fluences in the spheroidal liver, torus-shaped volumes were programmed to keep track of the particles (called tallies in MCNP), thereby simulating the rotation (see Fig. 2).

As illustrated in Fig. 2, which was drawn in Sabrina (31),⁷ every torus is positioned symmetrically around the vertical axis through the center of the spheroidal liver. To calculate the thermal flux field gradient near the edge of the liver model more accurately, tori with smaller radii are used. Note that tori at the vertical axis are spheres.

Using tori, only one calculation is needed in which the beam irradiates the liver from one direction. MCNP adds all the track lengths of the particles inside the torus volume and gives, when dividing by the volume of the torus, the flux. This averaging of the calculated flux over the whole

⁷ J. T. West III, SABRINA: An Interactive Three-Dimensional Geometry-Modeling Program for MCNP. Los Alamos National Laboratory Report LA10688M, 1986.

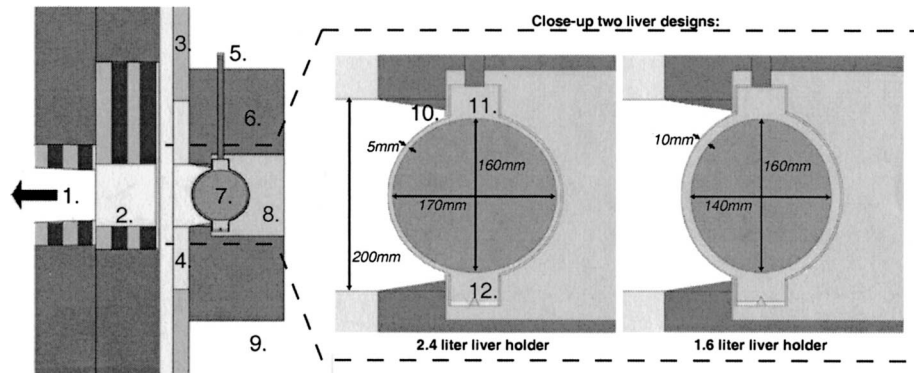


FIG. 3. Left: Lateral view of the final setup; Right (surrounded by dashed line): Enlarged side view of the two possible liver container setups. 1. Reactor core and filter. 2. Beam shutter with no collimator installed. 3. Wall containing boron. 4. Wall containing lithium. 5. Aluminum rotation axle attached to liver container. 6. Graphite reflector. 7. PMMA liver holder. 8. PMMA cube surrounding holder. 9. BNCT irradiation room. 10. Graphite cone. 11. Cylindrical part of PMMA holder for rotation and connecting the two halves (surrounded by Teflon for smooth rotation.) 12. Like 11 but also centered on Teflon cone.

torus is an excellent simulation of the flux distribution for the rotating liver. In fact, as a consequence, the flux becomes a time-averaged flux inside the rotating liver.

Note that the flux is uniform in the whole torus after each revolution, and the time it takes to make the flux uniform depends on the rotation speed of the liver.

Liver Irradiation Setup

The design concept for the setup to irradiate the extracorporeal liver does not require any changes to the existing patient treatment environment. The neutron source spectrum and source strength also do not need to be adapted. The liver setup itself must be portable and must be easy to install and remove. Furthermore, the design must be economical with regard to use of standard materials and components. To keep the liver cool, small jets of cold air directed toward the position of the organ will be used, which requires a precise control of the temperature. This feature must be installed in such a way that it does not disturb the neutron field.

The design has evolved from surrounding the liver container by water (good scatterer, moderator and coolant) toward a surrounding of solid material with the same characteristics. It appears that the solid surrounding results in a negligible difference in yield. However, it is easier to manufacture in comparison with something that must be watertight. After we performed many calculations with different materials and configurations and did further fine-tuning, we arrived at the final setup for irradiating a volume (liver) of 2.4 liters and 1.6 liters, respectively, as shown in Fig. 3. The derivation and reasoning for these two volumes are given in the next section.

Figure 3 is a collection of three geometrical plots from MCNP. On the left, a cross section of the latter part of the beam line showing the shutter and the wall of the BNCT irradiation room with the facility for the liver is given. Without installing any collimator, the beam diameter is 16 cm, thereby giving higher fluxes at the edges of the beam.

The spheroid-shaped container holding the liver is placed in a PMMA square cube with sides of 26 cm. The PMMA cube acts as a neutron scatterer, especially for the top and bottom of the spheroid. For back scattering, the cube is surrounded by pure graphite blocks (1.6 g/cm^3) with the entrance a graphite cone.

Each spheroid-shaped container for holding a liver is made from PMMA and consists of two equal parts that are connected after the liver is inserted. The advantages of PMMA are that it can be shaped easily, is non-toxic, behaves well at 4°C , will not be activated by the irradiation, and is transparent, which allows observation of the liver within the moving device. A disadvantage of PMMA is the production of γ rays due to the (n,γ) reaction from hydrogen. However, at the same time, the PMMA

can be used as buildup material for the thermal neutrons in a rather thin layer due to the high elastic scattering cross section of the same hydrogen. It has exactly the same effect as the skin and cranium, which moderate the epithermal neutrons in the BNCT treatment of brain tumors. In earlier designs for the 2.4-liter container, the wall of the PMMA container was the thickest (5 mm) at the equator and decreased to 2 mm toward the top and bottom of the spheroid. Although the neutron flux distribution could be tuned even better in this way, for engineering, we chose to have a constant PMMA thickness.

The liver sealed in a plastic bag will be delivered together with a conservation solution. After the bag is put into the container, the container will be filled as much as possible with liquid (water or more conservation solution). This serves to fill empty spaces to avoid any air gaps that would influence the irradiation field.

In this computational study, the liver composition and density of the modeled human are taken from ICRU Report 46 (32). The complete volume inside the container is modeled as liver tissue, which is comparable with water and the conservation solution. During the transport calculations, a conservatively chosen 15 ppm of ^{10}B is distributed homogeneously in the liver. From the brain studies, it is known that the thermal neutron flux at 7.3 cm depth in the brain will be 4% higher when there is only 7.5 ppm ^{10}B distributed homogeneously (33). Therefore, “conservatively” means that if the boron concentration in healthy liver tissue is lower than 15 ppm, the results will be somewhat better than presented in this study.

RESULTS

In this computational study, two optimal setups have been considered that represent the lower and the upper limits. The lower limit is an irradiation volume capacity of 1.6 liters; it is not expected that there will be livers, together with the necessary amount of conservation liquid (of the order of 100 ml), that are smaller than this volume. The upper limit, an irradiation volume capacity of 2.4 liters, is constrained by the existing beam characteristics.

Thermal Neutron Flux Distribution

In BNCT, three of the four major dose contributors are based on thermal neutron reactions. The thermal neutron flux is therefore the most characterizing parameter.

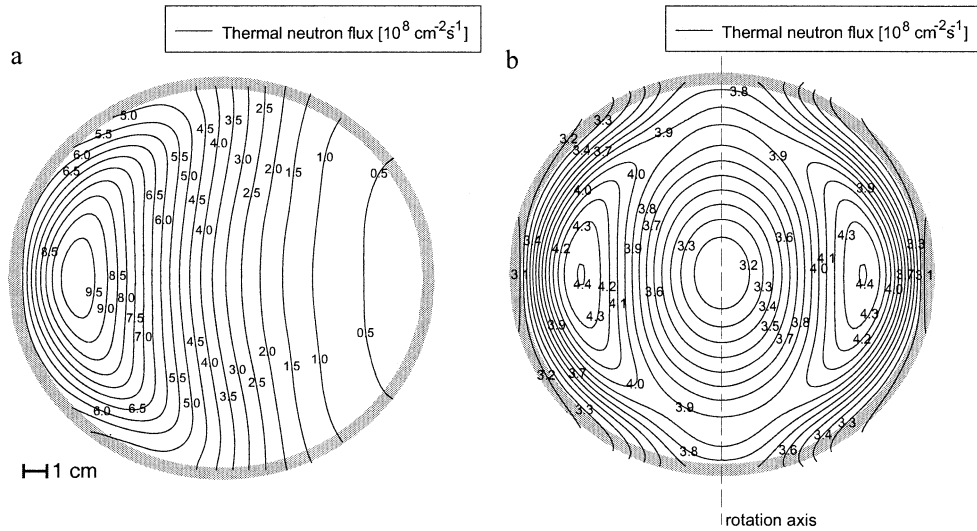


FIG. 4. Panel a: Thermal neutron flux inside the 2.4-liter container when irradiated from one side. Panel b: Thermal neutron flux with the container rotating.

Figure 4 shows thermal neutron flux distribution for the case of the 2.4-liter volume: an equatorial radius of 8.5 cm and a polar radius of 8.0 cm. Thermal neutrons are defined as neutrons with an energy below 0.414 eV. A proportionally sized image of the PMMA container is given as background to this contour plot. The statistical uncertainties in the MCNP results presented in this study are less than 1%.

Figure 4a gives the thermal neutron flux at the vertical cross section along the beam line if the container is stationary. The neutron beam is incident from the left; hence it is not surprising to see the highest flux values at the thermal peak positioned at the left side of the liver. In Fig. 4b, when the liver container rotates, the effect of this rotation on the flux distribution produces a more homogeneous field. Note that the gradient of the thermal neutron flux field in the left panel gives a disturbed view when compared with the right panel due to a different step size

in the contour lines. Clearly, from Fig. 4b, the thermal maximum is around $4.4 \times 10^8 \text{ cm}^{-2} \text{ s}^{-1}$ at 3 cm from the surface. Similar results can be seen in Fig. 5, where the thermal neutron flux contours are plotted for the 1.6-liter liver container. In this design, the loss of volume is exchanged for an more homogeneous thermal neutron field.

For the 2.4-liter container, the lowest thermal neutron fluxes are at the edge and at the center of the liver. Increasing the thermal neutron flux at the edges can be accomplished by more PMMA, which will scatter and slow down more epithermal neutrons. To compensate for the loss of thermal neutrons at the center, the equatorial diameter is decreased. The optimal dimensions turn out to be an equatorial radius of 7.0 cm and polar radius of 8.0 cm. The latter is directly related to the size of the beam. In fact, the orientation of the 1.6-liter spheroid is rotated when compared with the 2.4-liter container. Of course, this makes absolutely no difference for the inserted liver. Since Figs. 4 and 5 are 2D representations of a 3D model, it is necessary to give information on how the thermal neutron flux is distributed over the whole volume of the containers. Note that an area further away from the center describes a bigger torus volume than the same area closer to the center. Figure 6 shows the thermal neutron flux–volume histograms for both containers.

In 7% of the volume of the 2.4-liter container, the thermal neutron flux is between $3.3 \times 10^8 \text{ cm}^{-2} \text{ s}^{-1}$ and $3.4 \times 10^8 \text{ cm}^{-2} \text{ s}^{-1}$. In the 1.6-liter container, apart from the lowest interval, all thermal neutron flux intervals are more or less equal in filling the volume. The smaller width of the spectrum for the small container shows the greater homogeneity. Note that the lowest thermal neutron flux interval in the 2.4-liter container looks quite significant when shown as an iso-contour, as in Fig. 4b (region at the center), but is virtually negligible in terms of volume (1.1%). For what

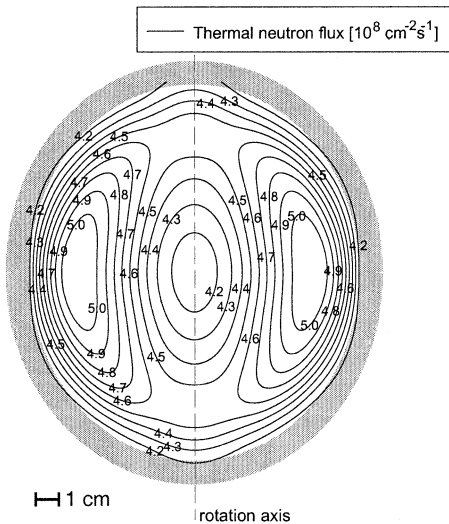


FIG. 5. Thermal neutron flux contours inside the 1.6-liter container.

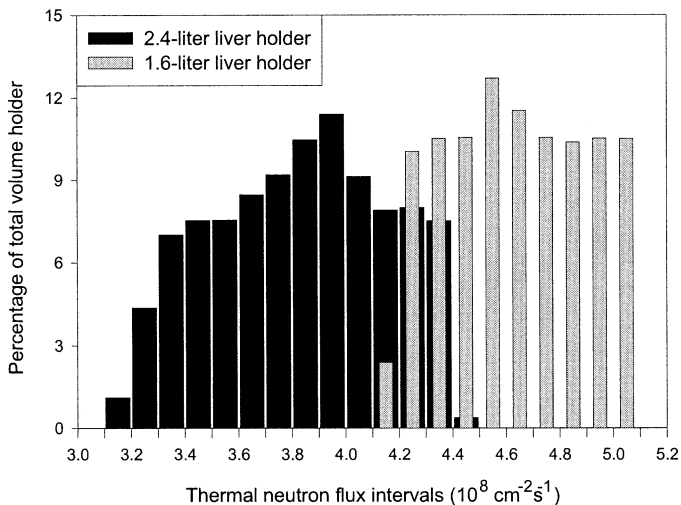


FIG. 6. Thermal neutron flux–volume histograms of the two liver containers.

it may be worth, the lowest thermal neutron fluxes are in the smallest volume fractions of the liver, which, it could be argued, increases the probability that there is no tumor in these volumes.

Irradiation Times

A summary of the results for both containers is given in Table 1. As well as the maximum and minimum thermal neutron fluxes, the irradiation time needed to deliver a fluence of $4 \times 10^{12} \text{ cm}^{-2}$ and the irradiation time needed to reach the defined upper limit of D_w of 15 Gy are also given. To calculate the weighted dose D_w , the weighting factors and the concentration (8 ppm) of ^{10}B in the healthy liver tissue from the Pavia case have been used.

To give insight into the composition of the various dose contributions, Table 2 gives an overview of the major physical dose components. The applied ^{10}B concentrations for healthy and tumor tissue are the ones reported for the first patient in Pavia.

Influence of the Materials

Small variations in the thermal neutron flux, up to 4% in certain positions within the liver, can be expected due to the position of the rotation axle. The influence of the sur-

rounding graphite blocks and cone gives 5% to 15% higher thermal neutron fluxes, according to the position within the liver. Although the surrounding PMMA is needed for scattering and buildup of thermal neutrons, its effect is due to the hydrogen and it therefore results in the production of photons. Near the center of both containers, around 8% of the total photon dose is due to photons produced in the PMMA. At the top and bottom of the containers, this number is around 30%. In absolute values, the photon dose rate at the bottom and top of the containers is two-thirds of the total photon dose rate at the center, being at the same time the minimum and maximum, respectively.

DISCUSSION

A single MCNP calculation with torus-shaped volumes to keep track of the particles enables the simulation of a rotating liver. A setup with inexpensive and easy-to-use materials has been designed and is presented here for the case of two extreme liver volumes: 1.6-liter and 2.4-liter containers.

These experiments and mathematical evaluations have been strongly stimulated by the pioneering work of Zonta, Pinelli and co-workers from Pavia (Italy). It was without doubt a success to achieve 4-year survival in a patient suffering from multiple liver metastases whose disease progressed after conventional chemotherapy. It is regrettable that the technical procedures and the physical basis as well as the clinical background have not yet been published in detail. Most of the information reported in this article regarding the Pavia case has been taken from conference proceedings (4, 23, 34, 35) and is based on oral public presentations^{3,8} and personal communications.²

Regarding the neutronics, the published work from Pavia (4, 23, 35) is based on a thermal column. Two other publications (9, 10) have investigated the possibility of an intracorporeal liver irradiation. All of this work is difficult to compare with the approach reported here, which can be best compared with a Finnish “epithermal” study (8). The Finnish work emphasizes the advantages of using epithermal neutrons in general when treating a large organ, and it ends

⁸ Eleventh World Congress on Neutron Capture Therapy, October 11–15, Boston, 2004.

TABLE 1
Characteristics of the Thermal Neutron Flux and Irradiation Times for the Two Liver Containers

	1.6-liter container	2.4-liter container
Thermal neutron flux ($\text{cm}^{-2} \text{ s}^{-1}$)		
Average:	4.7×10^8	3.8×10^8
Minimum:	4.1×10^8 (12% below average)	3.1×10^8 (20% below average)
Maximum:	5.1×10^8 (9% above average)	4.5×10^8 (17% above average)
Time limits (min)		
To deliver average thermal fluence of $4 \times 10^{12} \text{ cm}^{-2}$	142	175
To deliver D_w of 15 Gy in healthy tissue (+8 ppm ^{10}B)	138	155

TABLE 2
Calculated Dose Rates for Healthy and Tumor Tissue in the Two Liver Containers

	Total biologically weighted dose rate		Physical dose rates			
	\dot{D}_w tumor (Gy/h) (47 ppm ^{10}B)	\dot{D}_w healthy (Gy/h) (8 ppm ^{10}B)	\dot{D}_B (Gy/h) (8 ppm ^{10}B)	\dot{D}_n (Gy/h)	\dot{D}_p (Gy/h)	\dot{D}_γ (Gy/h)
	1.6 liters					
Minimum	23.7	5.2	0.9	0.1	0.3	2.2
Maximum	29.0	6.5	1.1	0.5	0.4	3.3
Average	26.5	6.0	1.0	0.3	0.3	2.8
2.4 liters						
Minimum	18.6	4.8	0.7	0.1	0.2	1.8
Maximum	25.4	5.8	0.9	0.5	0.3	2.9
Average	22.3	5.4	0.8	0.3	0.3	2.4

with the question as to what the influence of the irradiation setup would be, which is one of the objectives of the analysis presented in this paper.

In both liver holders, the desired thermal neutron fluence of $4 \times 10^{12} \text{ cm}^{-2} \pm 20\%$ can be reached in the required time frame. With respect to the weighted dose given to the liver, the predefined value of 15 Gy is exceeded. This is a very critical issue, because the suggestion made by Pinelli *et al.* in 2001 (23) was intended to describe a maximum in a small volume. In 2002, Pinelli reported that the patient treated in Pavia received a total weighted dose D_w of $8.6 \pm 0.5 \text{ Gy}$ (4) but did not specify how much volume of liver received this dose. The approach presented here probably leads to a more homogeneous distribution of all dose components inside the liver, which may not be an advantage with respect to the tolerance dose of the organ. This is unknown under the conditions used to irradiate an explanted organ. Animal experiments will be necessary to establish the tolerance dose to a healthy explanted liver after BPA infusion. The most suitable model would appear to be the pig, in which the organs are of similar size to those of humans.

Possible means to increase the thermal fluence include a further reduction of the beam γ rays and/or decreasing the highest thermal flux value in the liver. Decreasing the beam γ rays would require a new beam design, although it is doubtful that it would be possible to decrease the existing γ -ray component even further without affecting the epithermal neutron spectrum and flux. Decreasing the maximum thermal neutron flux at the thermal peak is impossible since this thermal peak is inherent to the use of an epithermal beam. Although it is feasible to shift the position of this peak slightly, the procedure is limited by its significant influence on the fluxes at the surface and near the center of the organ.

This computational study has achieved its objective and has led to a positive outcome, thus encouraging the next step in the project, which is to build the facility and start

a program of dosimetry measurements to validate the calculations.

The distribution of boron-10 throughout the irradiated liver must also be evaluated in detail to better determine the dose delivered to the healthy tissue. A first step has been undertaken by the clinical trial EORTC 11001 (13),⁶ which investigates the uptake of BPA in liver tissue and liver metastases.

In conclusion, the requirement for irradiating an extracorporal liver with BNCT using the epithermal neutron beam at the HFR Petten can be closely met. With the therapeutic requirement that the tolerance dose and ^{10}B concentrations allow a safe and effective treatment, extracorporal treatment of liver cancer by BNCT at the existing BNCT facility in Petten is feasible from the technical point of view.

ACKNOWLEDGMENTS

This work has been supported financially by the European Commission, contract no QLK3-CT-1999-01067.

Received: July 8, 2005; accepted: December 22, 2005

REFERENCES

1. A. Jemal, R. C. Tiwari, T. Murray, A. Ghafoor, A. Samuels, E. Ward, E. J. Feuer and M. J. Thun, Cancer statistics. *Cancer J. Clin.* **54**, 8–29 (2004).
2. J. Scheele, R. Stangl, A. Altendorf-Hofmann and F. P. Gall, Indicators of prognosis after hepatic resection for colorectal secondaries. *Surgery* **110**, 13–29 (1991).
3. D. J. Bentrem, R. P. DeMatteo and L. H. Blumgart, Surgical therapy for metastatic disease to the liver. *Annu. Rev. Med.* **56**, 139–156 (2005).
4. T. Pinelli, A. Zonta, S. Altieri, S. Barni, A. Braghieri, P. Pedroni, P. Bruschi, P. Chiari, C. Ferrari and C. Zonta, TAOOrMINA: From the first idea to the application to the human liver. In *Research and Development Neutron Capture Therapy* (W. Sauerwein, R. Moss and A. Wittig, Eds.), pp. 1065–1072. Monduzzi Editore, Bologna, 2002.

5. E. Wilkinson, An out-of-body experience. *Lancet Oncol.* **4**, 64 (2003).
6. L. Roveda, U. Prati, J. Bakeine, F. Trotta, P. Marotta, P. Valsecchi, A. Zonta, R. Nano, A. Facoetti and P. Pedroni, How to study boron biodistribution in liver metastases from colorectal cancer. *J. Chemother.* **16**, 15–18 (2004).
7. R. Nano, S. Barni, P. Chiari, T. Pinelli, F. Fossati, S. Altieri, C. Zonta, U. Prati, L. Roveda and A. Zonta, Efficacy of boron neutron capture therapy on liver metastases of colon adenocarcinoma: optical and ultrastructural study in the rat. *Oncol. Rep.* **11**, 149–153 (2004).
8. P. Kotiluoto and I. Auterinen, MCNP study for epithermal neutron irradiation of an isolated liver at the Finnish BNCT facility. *Appl. Radiat. Isot.* **61**, 781–785 (2004).
9. M. Suzuki, Y. Sakurai, S. Masunaga, Y. Kinashi, K. Nagata and K. Ono, Dosimetric study of boron neutron capture therapy with borocaptate sodium (BSH)/lipiodol emulsion (BSH/lipiodol-BNCT) for treatment of multiple liver tumors. *Int. J. Radiat. Oncol. Biol. Phys.* **58**, 892–896 (2004).
10. H. Koivunoro, D. L. Bleuel, U. Nastasi, T. P. Lou, J. Reijonen and K. N. Leung, BNCT dose distribution in liver with epithermal D-D and D-T fusion-based neutron beams. *Appl. Radiat. Isot.* **61**, 853–859 (2004).
11. W. Sauerwein, Principles and history of neutron capture therapy. *Strahlenther. Onkol.* **169**, 1–6 (1993).
12. A. Wittig, W. Sauerwein and J. Coderre, Mechanisms of transport of p-borono-phenylalanine through the cell membrane *in vitro*. *Radiat. Res.* **153**, 173–180 (2000).
13. W. Sauerwein and A. Zurlo, The EORTC Boron Neutron Capture Therapy (BNCT) Group: Achievements and future projects. *Eur. J. Cancer* **38**, S31–S34 (2002).
14. S. Obayashi, I. Kato, K. Ono, S. Masunaga, M. Suzuki, K. Nagata, Y. Sakurai and Y. Yura, Delivery of ^{10}B to oral squamous cell carcinoma using boronophenylalanine and borocaptate sodium for boron neutron capture therapy. *Oral Oncol.* **40**, 474–482 (2004).
15. I. Kato, K. Ono, Y. Sakurai, M. Ohmae, A. Maruhashi, Y. Imahori, M. Kirihaata, M. Nakazawa and Y. Yura, Effectiveness of BNCT for recurrent head and neck malignancies. *Appl. Radiat. Isot.* **61**, 1069–1073 (2004).
16. A. Z. Diaz, Assessment of the results from the phase I/II boron neutron capture therapy trials at the Brookhaven National Laboratory from a clinician's point of view. *J. Neurooncol.* **62**, 101–109 (2003).
17. H. Joensuu, L. Kankaanranta, T. Seppala, I. Auterinen, M. Kallio, M. Kulvik, J. Laakso, J. Vahatalo, M. Korttinen and S. Savolainen, Boron neutron capture therapy of brain tumors: Clinical trials at the Finnish facility using boronophenylalanine. *J. Neurooncol.* **62**, 123–134 (2003).
18. P. M. Busse, O. K. Harling, M. R. Palmer, W. S. Kiger, 3rd, J. Kaplan, I. Kaplan, C. F. Chuang, J. T. Goorley, K. J. Riley and R. G. Zamenhof, A critical examination of the results from the Harvard-MIT NCT program phase I clinical trial of neutron capture therapy for intracranial disease. *J. Neurooncol.* **62**, 111–121 (2003).
19. R. L. Moss, O. Aizawa, D. Beynon, R. Brugger, G. Constantine, O. Harling, H. B. Liu and P. Watkins, The requirements and development of neutron beams for neutron capture therapy of brain cancer. *J. Neurooncol.* **33**, 27–40 (1997).
20. H. Gray, *Anatomy of the Human Body*. Lea & Febiger, Philadelphia, 1918. [Thoroughly revised and re-edited by W. H. Lewis, New York, 2000; available online at <http://www.bartleby.com/107>]
21. M. Malago, G. Testa, A. Frilling, S. Nadalin, C. Valentini-Gamazo, A. Paul, H. Lang, U. Treichel and C. E. Broelsch, Cincinnati right living donor liver transplantation: An option for adult patients: Single institution experience with 74 patients. *Ann. Surg.* **238**, 853–862 (2003).
22. J. Rassow, W. Sauerwein, A. Wittig, E. Bourhis-Martin, K. Hideghéty and R. Moss, Advantage and limitations of weighting factors and weighted dose quantities and their units in boron neutron capture therapy. *Med. Phys.* **31**, 1128–1134 (2004).
23. T. Pinelli, S. Altieri, F. Fossati, A. Zonta, C. Ferrari, U. Prati, L. Roveda, S. Ngnitejeu Tata and D. M. Ferguson, Operative modalities and effects of BNCT on liver metastases of colon adenocarcinoma. In *Frontiers in Neutron Capture Therapy* (M. F. Hawthorne, K. Shelly and R. J. Wiersema, Eds.), pp. 1427–1440. Kluwer Academic, Plenum Publishers, New York, 2001.
24. J. A. Coderre, M. S. Makar, P. L. Micca, M. M. Nawrocky, H. B. Liu, D. D. Joel, D. N. Slatkin and H. I. Amols, Derivations of relative biological effectiveness for the high-LET radiations produced during boron neutron capture irradiation of the 9L rat gliosarcoma *in vitro* and *in vivo*. *Int. J. Radiat. Oncol. Biol. Phys.* **27**, 1121–1129 (1993).
25. G. M. Morris, J. A. Coderre, J. W. Hopewell, P. L. Micca, M. M. Nawrocky, H. B. Liu and A. Bywaters, Assessment of the response of the central nervous system to boron neutron capture therapy using a rat spinal cord model. *Radiation Oncol.* **30**, 249–255 (1994).
26. H. Fukuda, J. Hiratsuka, C. Honda, T. Kobayashi, K. Yoshino, H. Karashima, J. Takahashi, Y. Abe, K. Kanda and M. Ichihashi, Boron neutron capture therapy of malignant melanoma using ^{10}B -parabornophenylalanine with special reference to evaluation of radiation dose and damage to the normal skin. *Radiat. Res.* **138**, 435–442 (1994).
27. D. E. Wessol, R. S. Babcock, F. J. Wheeler, G. J. Harkin, L. L. Voss and M. W. Frandsen, *BNCT-Rtpe: BNCT Radiation Treatment Planning Environment User's Manual*, Version 2.2, 1997. [Available online at <http://id.inel.gov/rtp-manual/sec00.html>]
28. D. E. Wessol, C. A. Wemple, F. J. Wheeler, M. T. Cohen, M. B. Rossmeier and J. J. Cogliati, *SERA: Simulation Environment for Radiotherapy Applications User's Manual*, version 1C0, 1999. [Available online at <http://www.cs.montana.edu/~bnct/manual/sec00.html>]
29. R. Zamenhof, E. Redmond, G. Solares, D. Katz, K. Riley, S. Kiger and O. Harling, Monte Carlo-based treatment planning for boron neutron capture therapy using custom-designed models automatically generated from CT data. *Int. J. Radiat. Oncol. Biol. Phys.* **35**, 383–397 (1996).
30. J. F. Briesmeister, Ed., *A General Monte Carlo N-Particle Code*, version 4C. Report LA-13079-M, Los Alamos National Laboratory, Los Alamos, NM, 2000.
31. K. A. Van Riper, New features in Sabrina. In *Radiation Protection for our National Priorities*, pp. 316–323. American Nuclear Society, La Grange Park, IL, 2000.
32. ICRU, *Photon, Electron, Proton and Neutron Interaction Data for Body Tissues*. Report 46, International Commission on Radiation Units and Measurements. Bethesda, MD, 1992.
33. S. J. Ye, Boron self-shielding effects on dose delivery of neutron capture therapy using epithermal beam and boronophenylalanine. *Med. Phys.* **26**, 2488–2493 (1999).
34. A. Zonta, U. Prati, L. Roveda, S. Zonta, C. Ferrari and C. Zonta, Clinical lessons from the first applications of BNCT on unresectable liver metastases. In *Europhysics Conference Abstracts* (A. Fontana, G. Viesti and A. Zenoni, Eds.), pp. 97–98. European Physical Society, Pavia, 2005.
35. T. Pinelli, S. Altieri, F. Fossati, A. Zonta, D. Cossard, U. Prati, L. Roveda, G. Ricevuti and R. Nano, Development of a method to use boron neutron capture therapy for diffused tumours of liver (TA-ORMINA project). In *Cancer Neutron Capture Therapy* (Y. Mishima, Ed.), pp. 783–794. Plenum Press, New York, 1996.